Science Signaling
AAAS

www.sciencesignaling.org/cgi/content/full/4/182/ra46/DC1

Supplementary Materials for

The Deacetylase SIRT1 Promotes Membrane Localization and Activation of Akt and PDK1 During Tumorigenesis and Cardiac Hypertrophy

Nagalingam R. Sundaresan, Vinodkumar B. Pillai, Don Wolfgeher, Sadhana Samant, Prabhakaran Vasudevan, Vishwas Parekh, Hariharasundaram Raghuraman, John M. Cunningham, Madhu Gupta, Mahesh P. Gupta*

*To whom correspondence should be addressed. E-mail: mgupta@surgery.bsd.uchicago.edu

Published 19 July 2011, *Sci. Signal.* **4**, ra46 (2011)
DOI: 10.1126/scisignal.2001465

The PDF file includes:

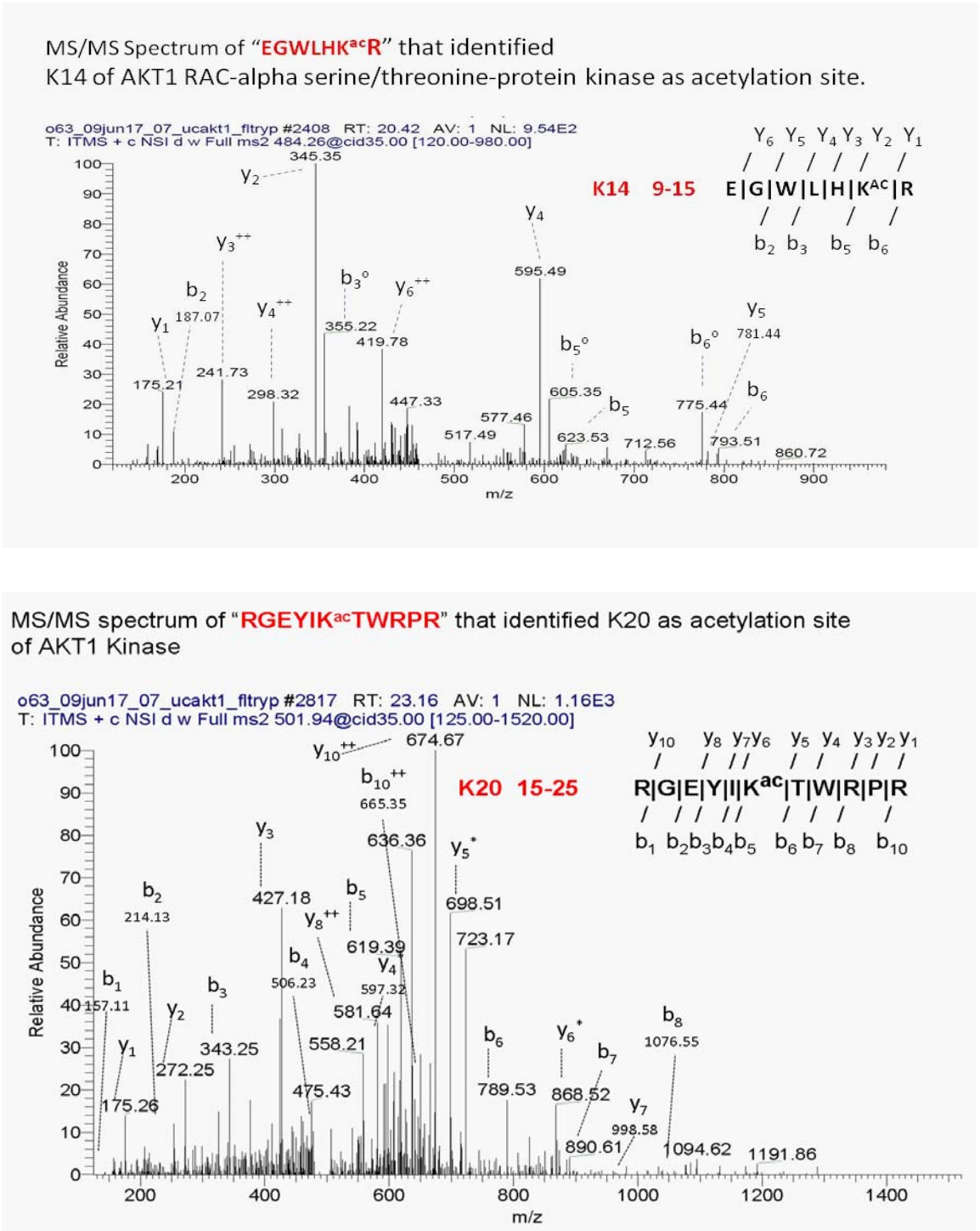

Fig. S1. Akt is acetylated at Lys[14] and Lys[20] in the PH domain. Annotation of representative tandem mass spectra of trypsin-digested Akt, depicting acetylation of Lys[14] (K14) (top panel) and Lys[20] (K20) (bottom panel).

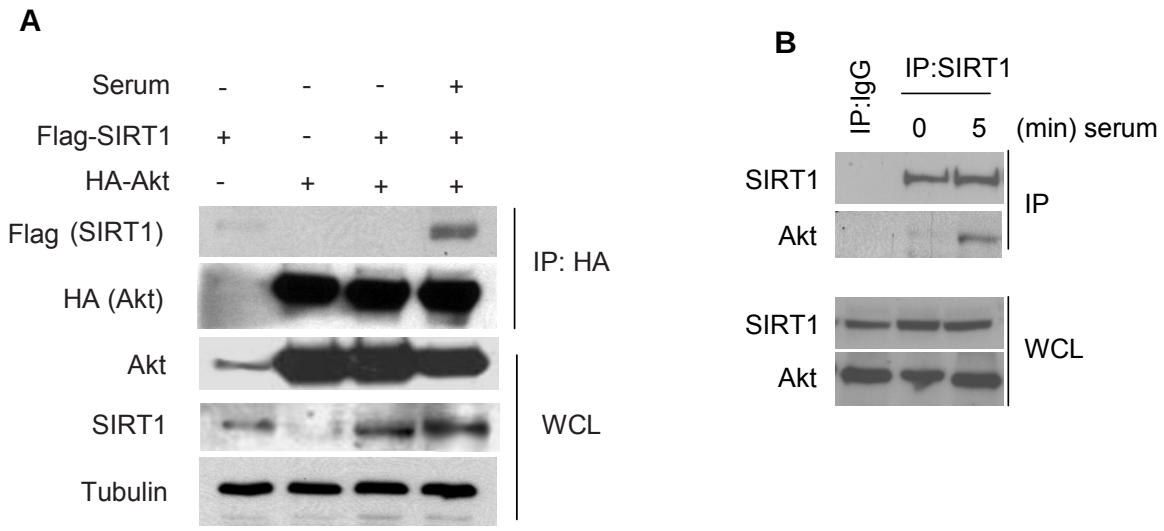

fig. S2. SIRT1 binds to Akt under growth-promoting conditions. (**A**) HEK293T cells expressing the indicated proteins were serum starved or maintained in serum-media overnight. Immunoprecipitated Akt was immunoblotted for coprecipitated SIRT1. N=2 experiments. (**B)** Cells were serum starved overnight and then stimulated with serum for 5 min. Immunoprecipitated SIRT1 was immunoblotted for coprecipitated Akt. N=3 experiments.

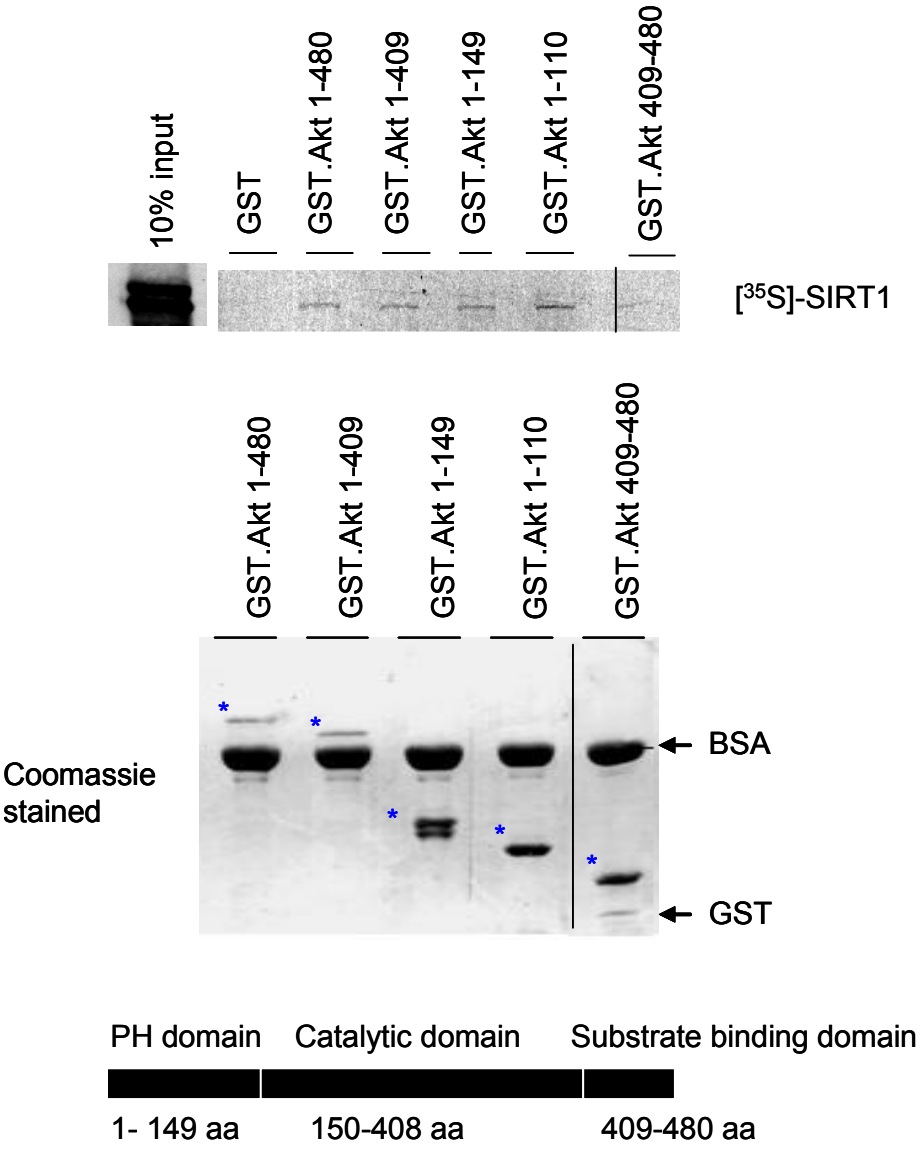

fig. S3. SIRT1 binds to the PH domain of Akt. GST pull-down assay showing interaction of [^{35}S]-SIRT1 with various GST-Akt fragments (upper). Coomassie blue-stained blot showing synthesis of different GST-Akt fragments (marked with asterisks) (middle). N = 2 experiments. Schematic representation of the different domains of Akt (bottom).

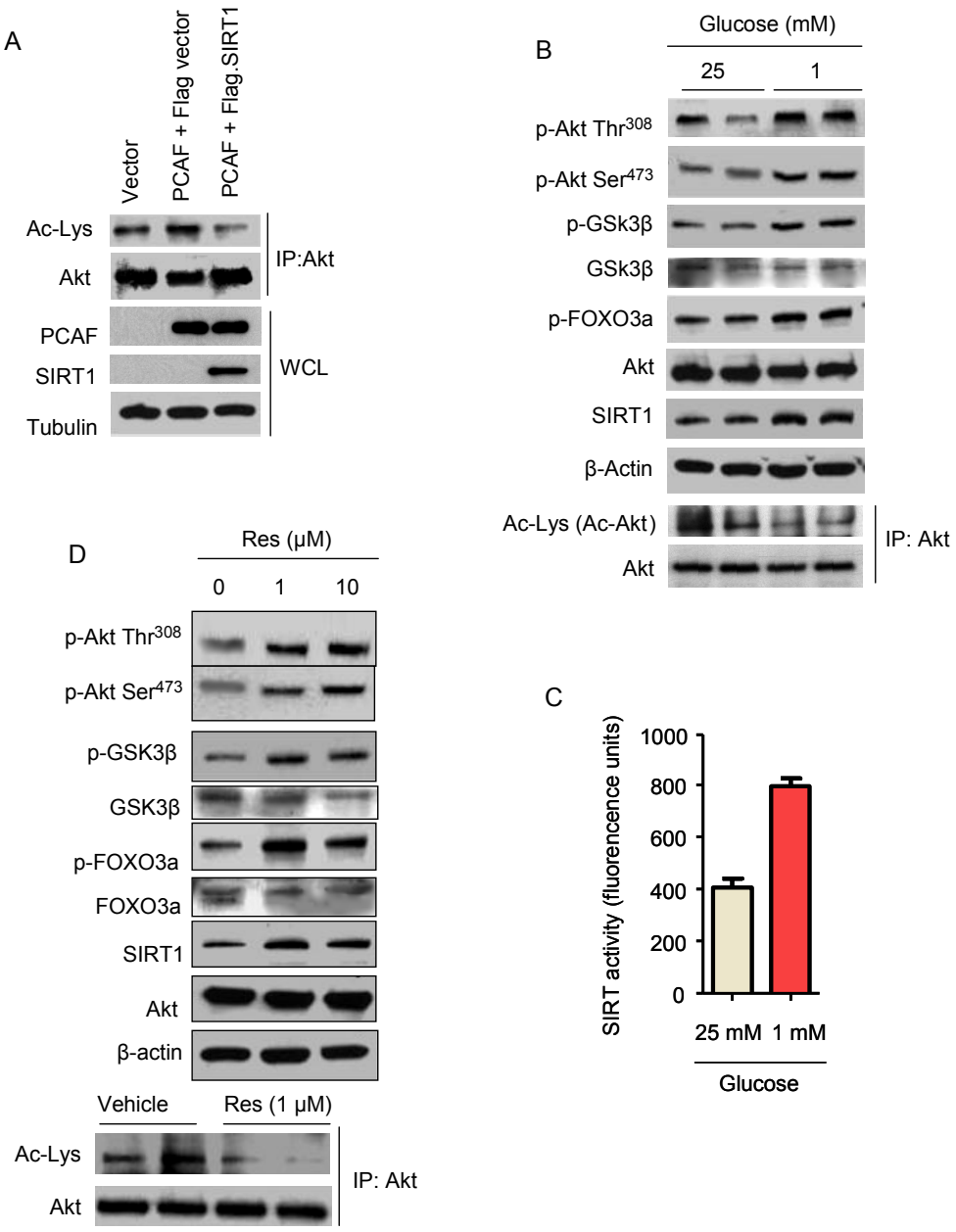

fig. S4. SIRT1 deacetylates and activates Akt in cells. (**A**) The acetylation status of endogenous Akt immunoprecipitated from HEK293T cells expressing the indicated proteins. (**B**) Akt phosphorylation was induced by placing growing cells in a limited glucose medium. HeLa cells were cultured in media containing 1 mM or 25 mM glucose overnight. The acetylation status of Akt was determined. (**C**) High glucose concentrations inhibit the deacetylase activity of SIRT1. SIRT1 was immunoprecipitated from cells grown in high (25 mM) or low (1 mM) glucose medium. The activity of SIRT1 was determined by the SIRT1 deacetylase Fluorometric assay kit (Cyclex). (**D**) HeLa cells were grown in complete media and treated with two different doses (1 or 10 μM) of resveratrol overnight. Acetylation of Akt was reduced in resveratrol-treated cells. N=2 experiments.

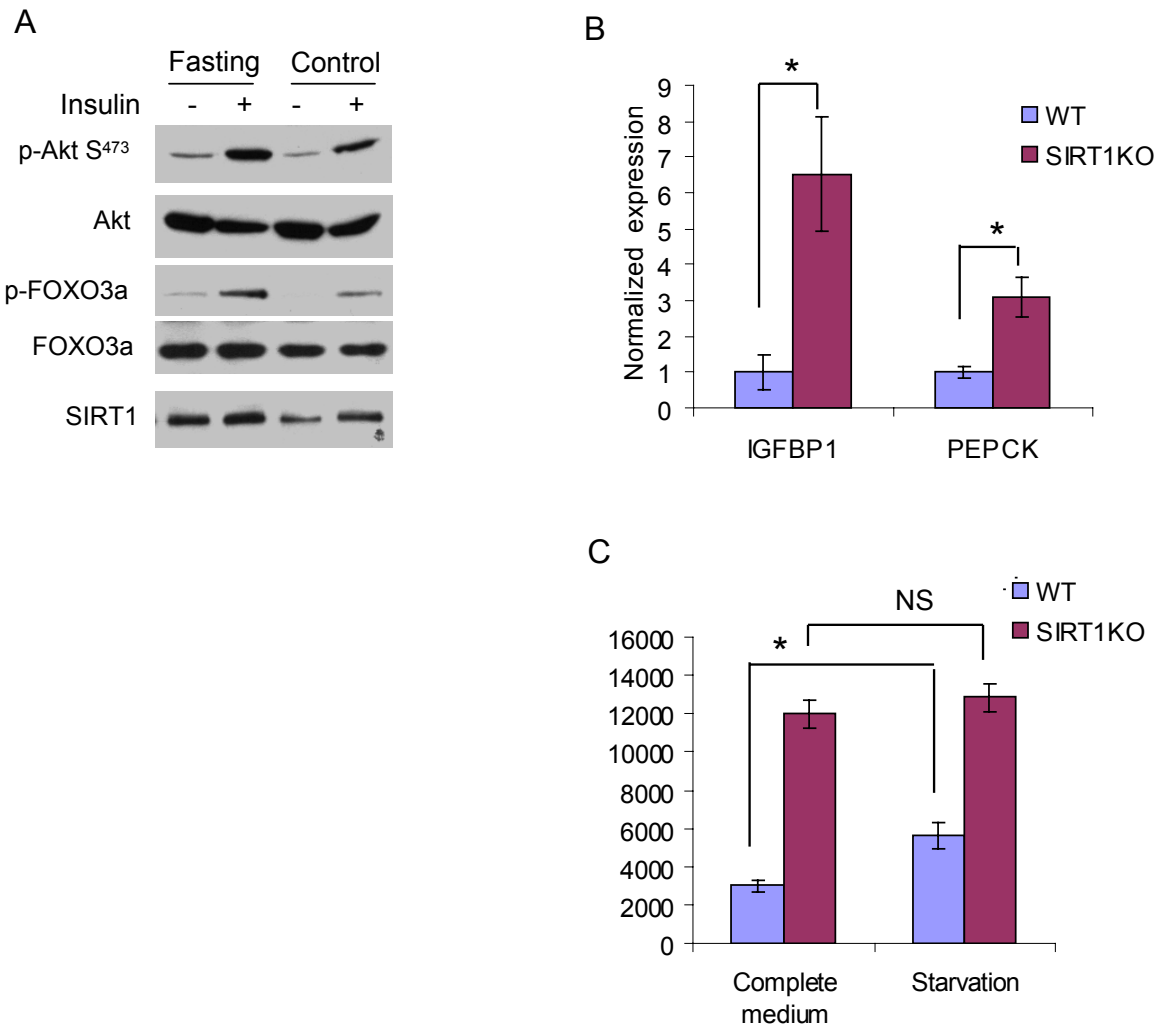

fig. S5. SIRT1-depleted cells show increased FOXO transcriptional activity. (**A**) Fasting promotes phosphorylation of Akt and FOXO3a under growth conditions. Mice fed ad libitum or fasted overnight were injected with insulin (0.75 units/kg). Skeletal muscle was harvested 30 min after injection and immunoblotted for the indicated proteins. N=3 (**B)** SIRT1-KO mice show increased abundance of mRNAs encoding PEPCK and IGFBP1 as quantified by real time PCR analysis. Values are means ± SE. N=6 mice per group. (**C)** SIRT1-KO fibroblasts show increased transcriptional activity of a FOXO-dependent reporter gene both in growth conditions (complete media) and growth factor-depleted conditions (starvation). FOXO transcriptional activity was measured with a FOXO-responsive promoter and luciferase reporter gene. FOXO transcriptional activity was increased in starved wild-type cells. However, no change in FOXO transcriptional activity was observed between starved SIRT1-KO cells or those maintained in complete media, suggesting that Akt-mediated inhibition of FOXO activity is blunted in SIRT1-KO cells. N=3 sets of cells.

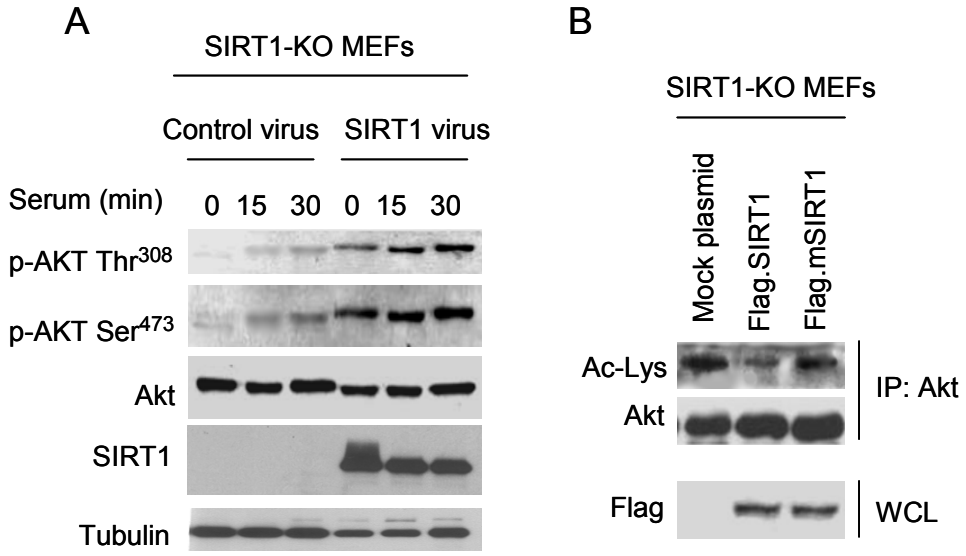

fig. S6. SIRT1 overexpression rescues phosphorylation of Akt in SIRT1-KO cells. (**A**) SIRT1-deficient MEFs infected with control or SIRT1-expressing adenovirus vectors were stimulated with serum for different time periods. Akt phosphorylation was determined by immunoblotting. N=2 experiments. (**B)** SIRT1-deficent MEFs grown in serum medium were transfected with plasmids expressing wild-type or mutant SIRT1 (mSIRT1). The acetylation status of immunoprecipitated Akt was determined by immunoblotting. N=2 experiments.

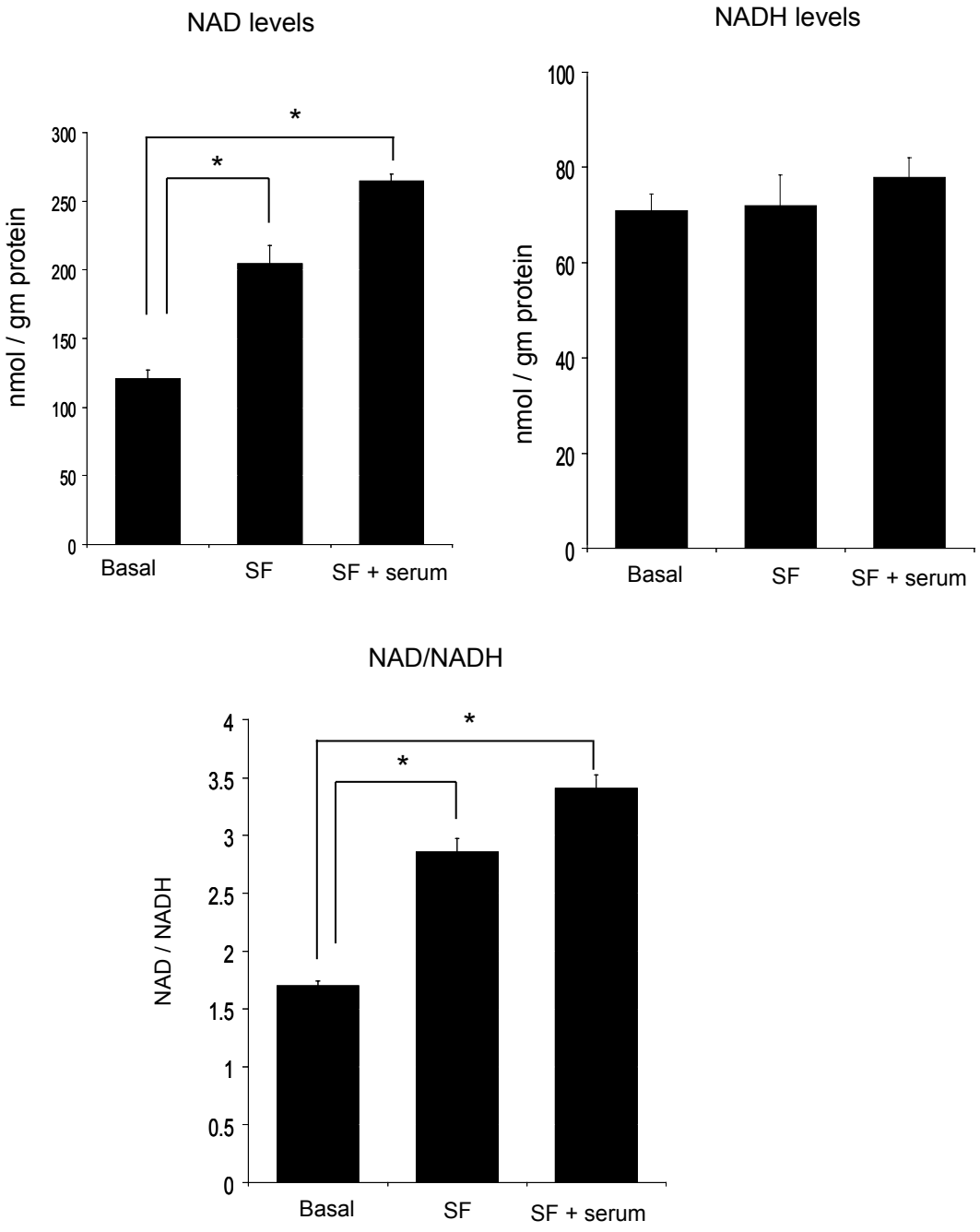

fig. S7. Growth factor treatment of cells increases the NAD/NADH ratio. HeLa cells grown to 70% confluence in complete medium were serum starved for 24 hours and treated with 10% FBS for 5 min. Cells were harvested and NAD and NADH concentrations were estimated with the Amplite NAD-NADH assay kit. Values are means ± SE; *P<0.05 N=3 sets of cells.

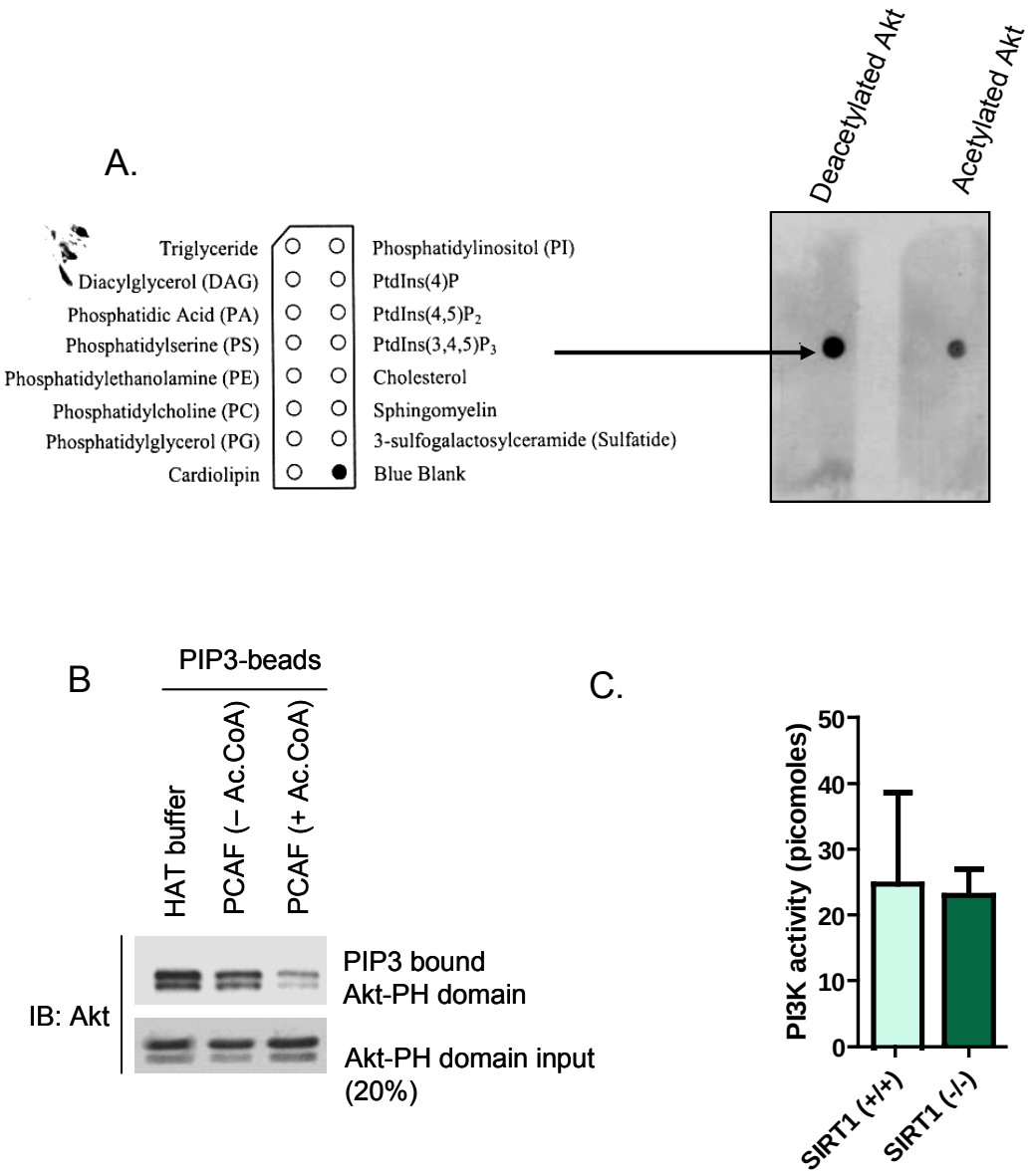

fig. S8. Acetylation specifically alters the binding ability of Akt to PIP_3. (**A**) The binding ability of acetylated or deacetylated Akt to immobilized lipids was assessed by a protein-lipid overlay assay. Nitrocellulose membranes spotted with different membrane lipids were incubated with acetylated or deacetylated Akt. Bound Akt to lipids was detected by immunoblotting with anti-Akt antibody. N=2 experiments. (**B**) Acetylation of the PH domain inhibits Akt binding to PIP_3. GST-Akt-PH domain was acetylated by PCAF in the absence or presence of Ac-CoA. Acetylated or non-acetylated GST-Akt-PH domain proteins were incubated with PIP_3 agarose beads. The binding of Akt-PH domain to PIP_3 beads was determined by immunoblotting. N=2 experiments. (**C**) SIRT1 does not change the activity of PI3K. Wild-type or SIRT1-deficient MEFs were serum starved overnight and induced with IGF-1 for 15 min. PI3K activity was assessed in cell lysates with the Echelon PI3K activity assay kit. Values are means ± SE. N = 5 sets of MEFs.

K495Ac VLKacGEIPWSQELRPEAK

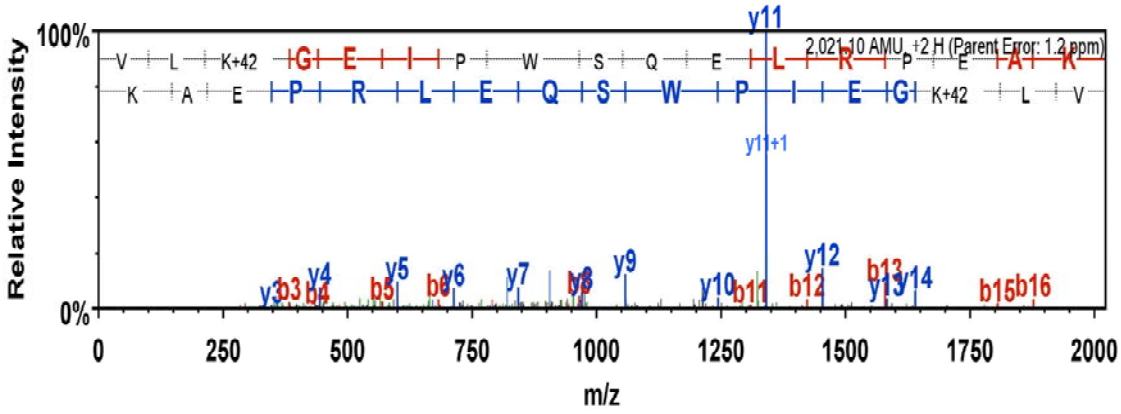

K534Ac TYYLMDPSGNAHoxKac

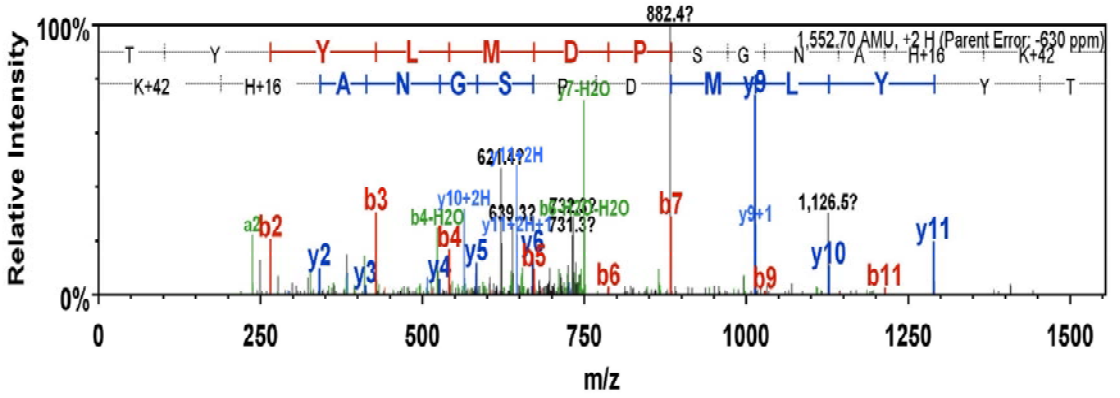

fig. S9. The PH domain of PDK1 is acetylated at Lys[495] and Lys[534]. Annotation of representative tandem mass spectra of trypsin-digested PDK1, indicating acetylation of two lysine residues in the PH domain.

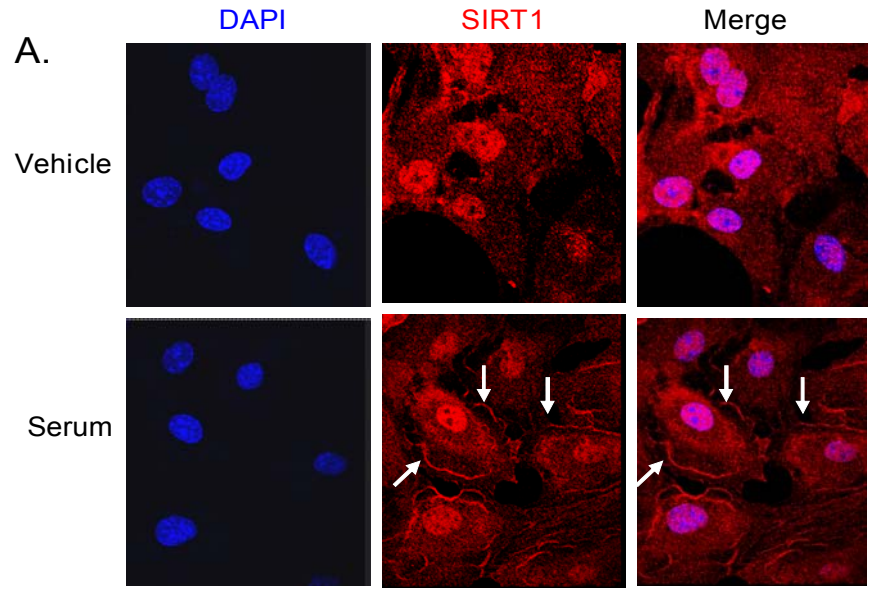
A.
DAPI
SIRT1
Merge
Vehicle
Serum

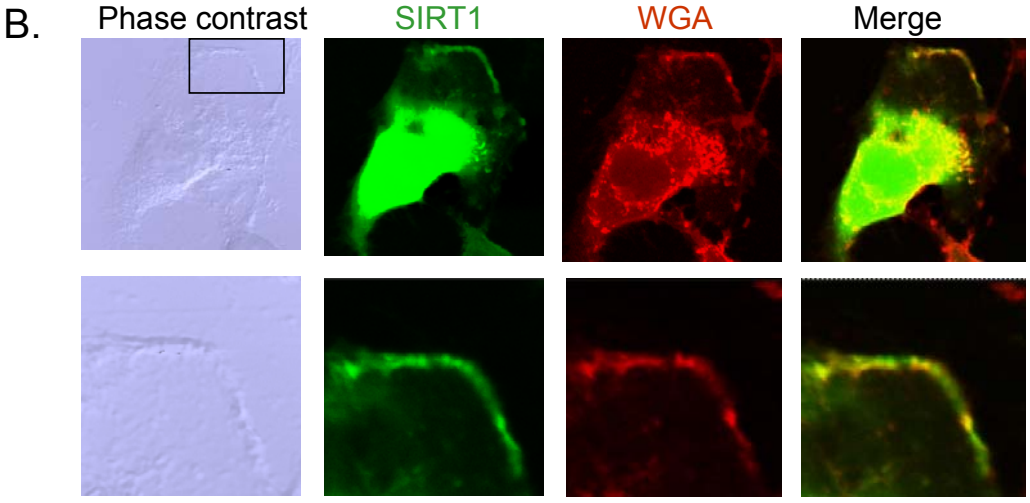
B.
Phase contrast
SIRT1
WGA
Merge

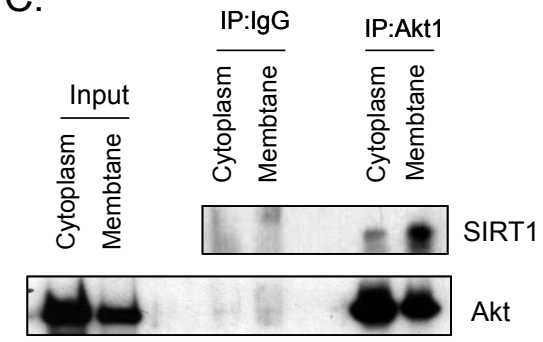
C.
IP:IgG
IP:Akt1
Input
Cytoplasm
Membtane
Cytoplasm
Membtane
Cytoplasm
Membtane
SIRT1
Akt

fig. S10. SIRT1 localizes to the plasma membrane under growth-promoting conditions. (**A**) PC3 cells were stimulated with serum for 15 min and immunostained with anti-SIRT1 antibody. Membrane localization of SIRT1 (arrows) was visualized by confocal microscopy. N= 2. (**B**) HeLa cells overexpressing SIRT1 were immunostained for SIRT1 and for the membrane marker wheat germ agglutinin (WGA). Membrane localization of SIRT1 was examined by confocal microscopy. Square on the top panel indicates the leading edge of cells magnified in lower panels, which show membrane localization of SIRT1 in the leading edge of HeLa cells. N=2 sets of cells. (**C**) Membrane and cytoplasmic fractions of serum-stimulated PC3 cells were examined for immunoprecipitation of SIRT1 with Akt. SIRT1 coprecipitated with Akt from the membrane fraction. N= 2.

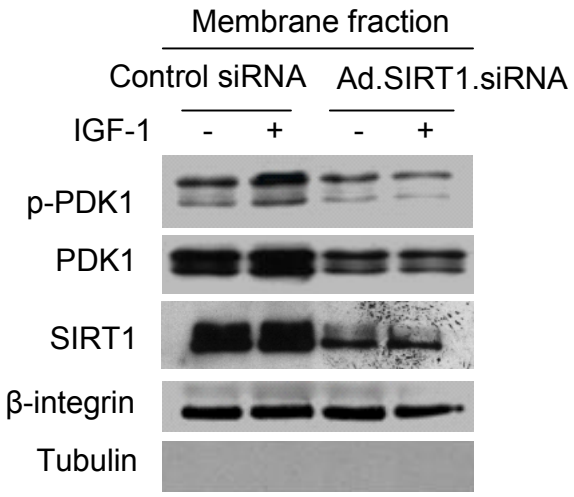

fig. S11. SIRT1-deficient PC3 cells do not show IGF-1-induced phosphorylation of PDK1. Cells expressing SIRT1-specific shRNA were serum starved overnight and treated with IGF-1 for 15 min. Membrane fractions were prepared and analyzed by immunoblotting.

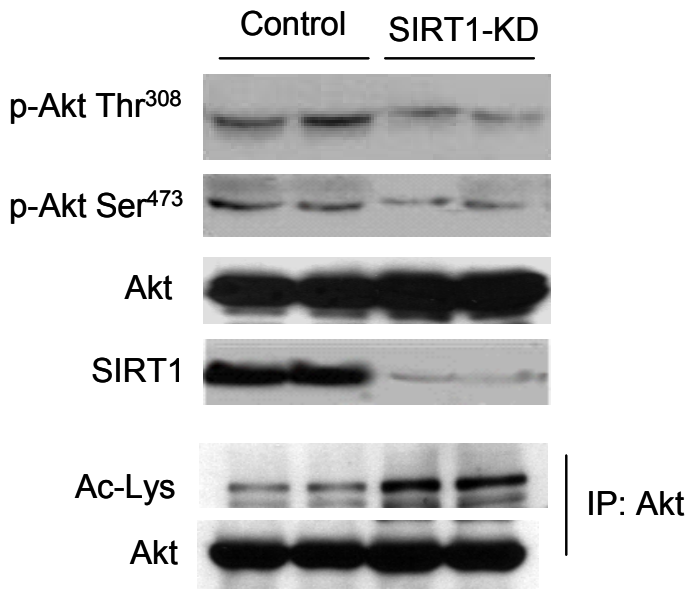

fig. S12. SIRT1-deficient PC3 cells show reduced activation of Akt. Immunoblot showing abundance of phosphorylated Akt and acetylated Akt in SIRT1-knockdown (SIRT1-KD) PC3 cells from Fig. 9A. N=2 sets of cells.

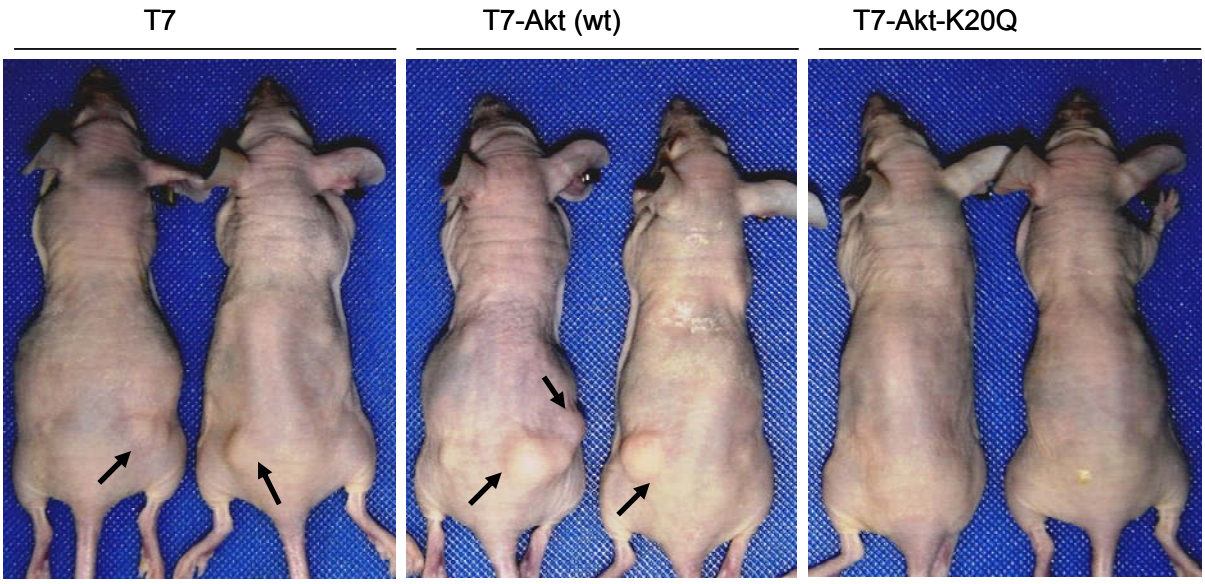

fig. S13. Lys^{20} acetylation inhibits the tumorigenic activity of Akt. HeLa cells stably expressing T7 tag alone, wild-type T7-Akt, or T7-K20Q mutant were injected into nude mice (n=6 mice per group) and monitored for tumor development (black arrow). Pictures were taken 8 weeks after injection.

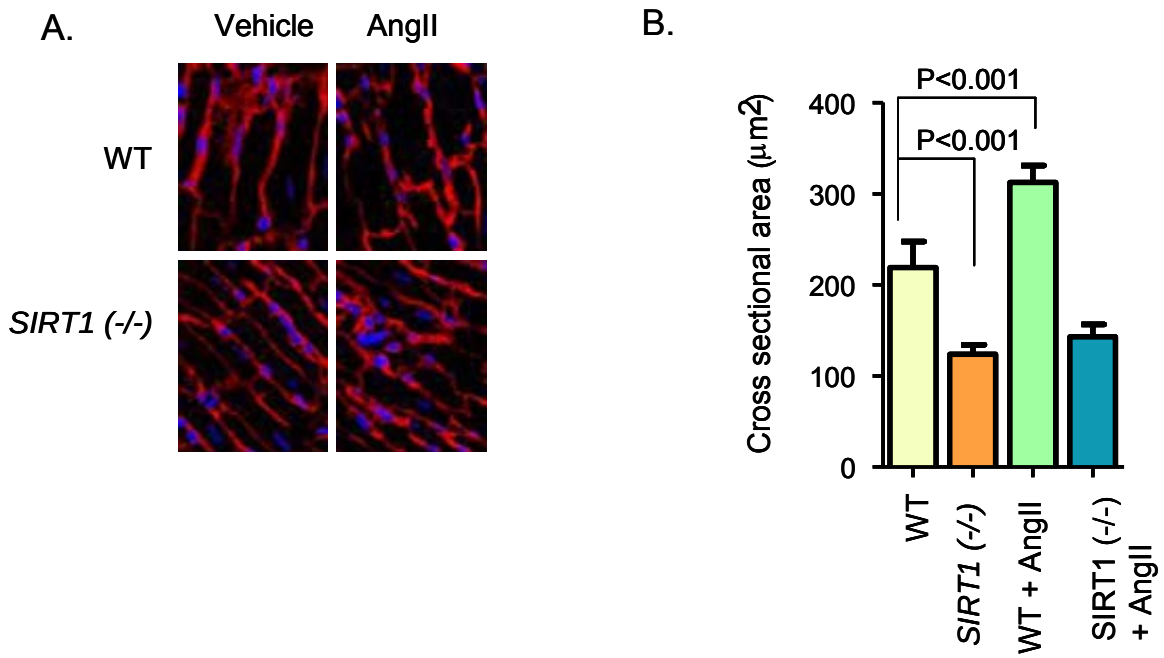

fig. S14. *SIRT1*$^{-/-}$ mice show reduced AngII-mediated cardiac hypertrophy. (**A**) Representative heart sections to show cardiomyocyte size in wild-type (WT) and *SIRT1*$^{-/-}$ mice treated with AngII to induce hypertrophy. (**B**) Quantification of cardiomyocyte cross-sectional area in AngII-treated WT and *SIRT1*$^{-/-}$ mice. Values are means ± SE. N = 6 mice per group.

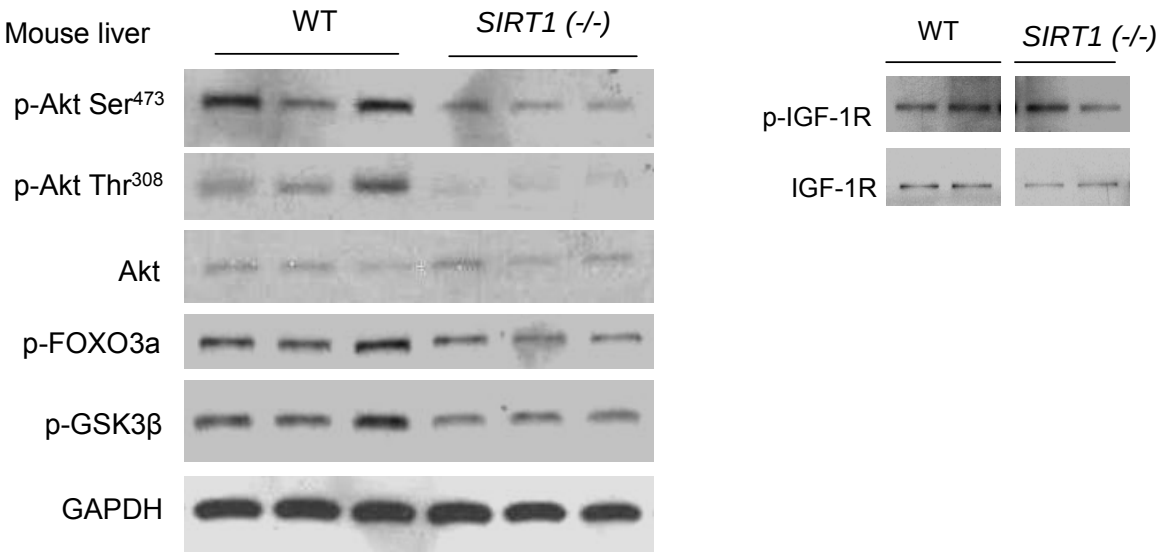

fig. S15. *SIRT1*$^{-/-}$ mouse liver shows reduced Akt phosphorylation. Immunoblots showing the abundance of different proteins in the livers of WT and *SIRT1*$^{-/-}$ mice. N=4 mice per group.

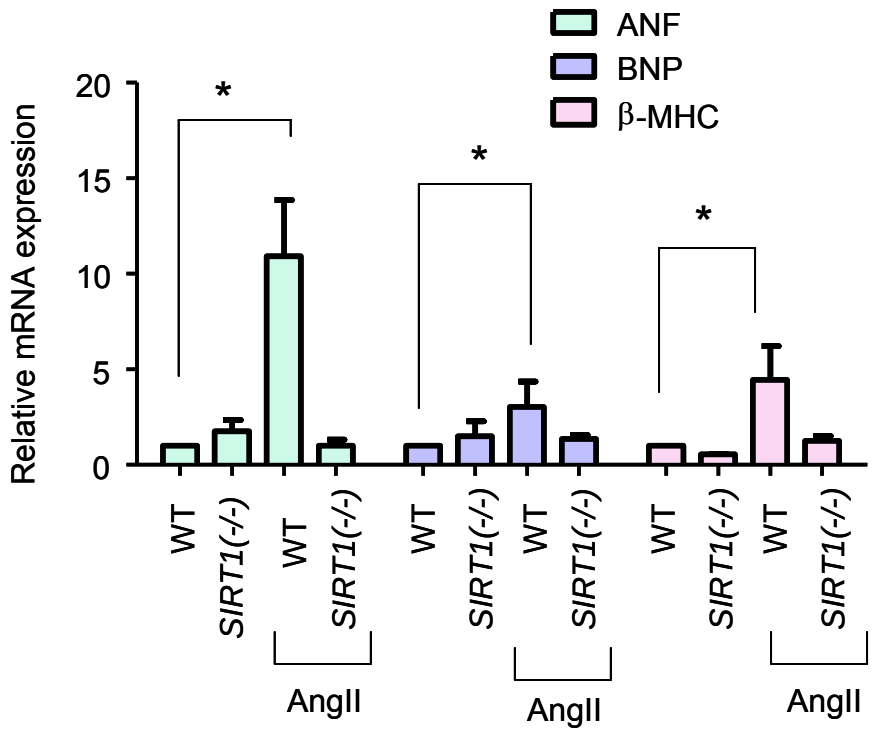

fig. S16. AngII infusion fails to induce hypertrophic markers in *SIRT1* $^{-/-}$ mice. Abundance of mRNAs encoding ANF, BNP, and β-MHC was assessed in heart samples from control (WT) and *SIRT1* $^{-/-}$ mice treated with AngII to induce hypertrophy by real-time PCR. Values are means ± SE. N=6-8 hearts per group. *P< 0.001.

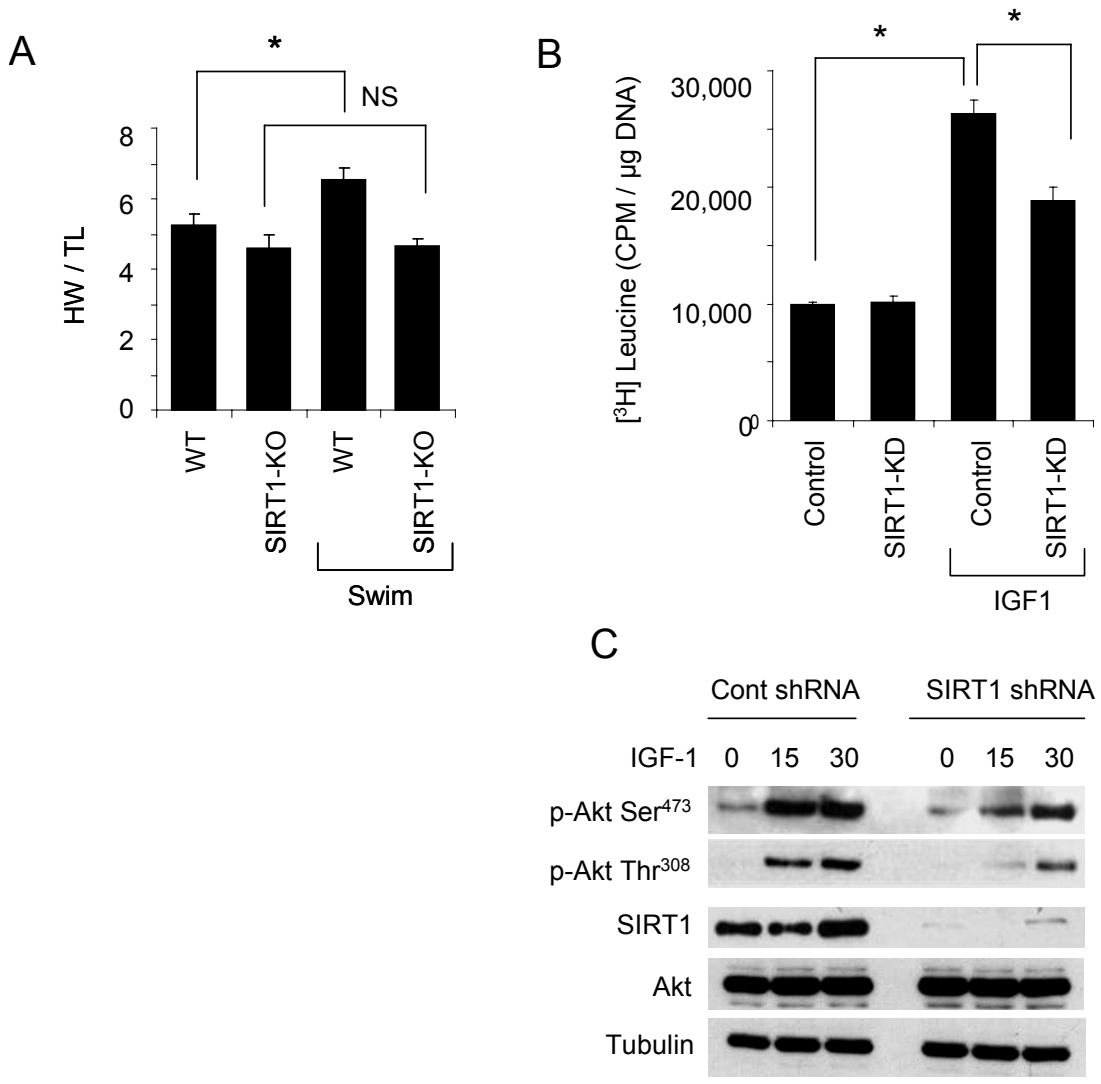

fig. S17. SIRT1 deficiency blocks the development of physiologic hypertrophy. (**A**) Wild-type and SIRT1-KO mice were subjected to forced swimming exercise for 8 weeks, 1 hr/day, 7 days a week.. Cardiac hypertrophy was determined by measuring the heart weight (HW)/ tibia length (TL) ratio. Values are means ± SE. N=8 mice per group. *P< 0.01; NS; not significant. **(B)** Control neonatal rat cardiomyocytes or those expressing SIRT1-specific shRNA were induced with IGF-1 (100 nM) for 48 hours. Hypertrophy of cardiomyocytes was determined by measuring [^{3}H]-leucine incorporation into total cellular protein. **(C)** Immunoblot showing reduced activation of Akt in SIRT1 knockdown neonatal rat cardiomyocytes.

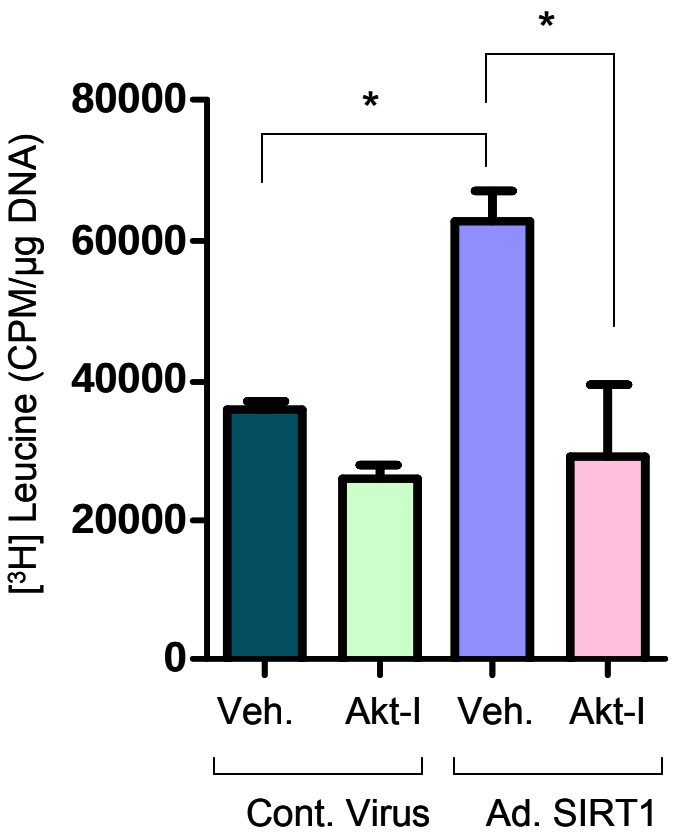

fig. S18. The Akt inhibitor triciribine blocks SIRT1-mediated hypertrophy of cardiomyocytes. Neonatal rat heart myocytes overexpressing SIRT1 were treated with the Akt inhibitor triciribine (Akt-I; 2 µM) or vehicle (Veh) for 36 hours. Cardiomyocyte hypertrophy was determined by measuring incorporation of [^{3}H]-leucine into total cellular proteins. Values are means ± SE. N = 5 experiments. * P< 0.001.

Table S1: Relative stoichiometry of acetylation of the PH domain of Akt.

Observed	Mr(expt)	Mr(calc)	Delta	Miss	Sequence	Intensity	MS Scan
463.7500	925.4854	924.4930	0.9925	1	K.EGWLHKR.G (Ions score 23)	52927.10	1166
484.2588	966.5031	966.5035	-0.0004	1	K.EGWLH**K_{Ac}**R.G Acetyl (**K14Ac**) (Ions score 21)	60910.90	2406
AKT1 K14Ac					Total Ion Intensity (Non-Ac + Ac)	**113838.00**	
					Relative Stoichiometry of AKT1 K14Ac (Ac/(Non-Ac + Ac))	**53.51%**	
436.5700	1306.6882	1304.6989	1.9892	1	R.GEYIKTWRPR.Y (Ions score 18)	26211.10	2322
674.3610	1346.7075	1346.7095	-0.0020	1	R.GEYI**K_{Ac}**TWRPR.Y Acetyl (**K20Ac**) (Ions score 12)	26439.10	3321
AKT1 K20Ac					Total Ion Intensity (Non-Ac + Ac)	**52650.20**	
					Relative Stoichiometry of AKT1 K14Ac (Ac/(Non-Ac + Ac))	**50.22%**	